Collective Decision Making in Bacterial Viruses

Joshua S. Weitz,*† Yuriy Mileyko,* Richard I. Joh,† and Eberhard O. Voit‡§
*School of Biology, †School of Physics, ‡School of Biomedical Engineering, and §Integrative BioSystems Institute, Georgia Institute of Technology, Atlanta, Georgia

ABSTRACT For many bacterial viruses, the choice of whether to kill host cells or enter a latent state depends on the multiplicity of coinfection. Here, we present a mathematical theory of how bacterial viruses can make collective decisions concerning the fate of infected cells. We base our theory on mechanistic models of gene regulatory dynamics. Unlike most previous work, we treat the copy number of viral genes as variable. Increasing the viral copy number increases the rate of transcription of viral mRNAs. When viral regulation of cell fate includes nonlinear feedback loops, very small changes in transcriptional rates can lead to dramatic changes in steady-state gene expression. Hence, we prove that deterministic decisions can be reached, e.g., lysis or latency, depending on the cellular multiplicity of infection within a broad class of gene regulatory models of viral decision-making. Comparisons of a parameterized version of the model with molecular studies of the decision structure in the temperate bacteriophage λ are consistent with our conclusions. Because the model is general, it suggests that bacterial viruses can respond adaptively to changes in population dynamics, and that features of collective decision-making in viruses are evolvable life history traits.

INTRODUCTION

Bacterial viruses (i.e., bacteriophages or phages) can be classified based on their life histories into two broad categories: virulent and temperate (1,2). Virulent phages possess two life history stages: an extracellular stage, in which a metabolically inactive virion passively diffuses in the environment; and an intracellular stage, in which the viral genome redirects transcription and translation leading to virion production and cell lysis. In contrast, once temperate phages infect host cells, they can either kill the host cell, thereby releasing viral progeny, or integrate their genetic material with that of their bacterial host. Once the viral genome of a temperate phage has integrated, the bacterium is referred to as a lysogen. In the lysogenic stage, minimal transcription and translation of viral proteins occurs and the viral genome (i.e., prophage) is transmitted vertically. Later, induction of the prophage can occur and the virus can reenter the lytic pathway. The choice of whether to lyse a host cell or enter a latent state upon infection as well as the mechanisms of prophage induction have been extensively studied in temperate phages. Analysis of the molecular mechanisms underlying the lysis versus lysogeny pathways has formed the basis for formative work on gene regulation (3). The study of the lysis-lysogeny switch in λ-phage has become a model system for understanding how temperate phages decide the means by which they exploit hosts (4–15).

Nearly all theoretical studies of temperate phage decision dynamics have claimed that switching between alternative pathways depends on some change in environmental conditions or some other random process inherent to the virus (6,7,10,16). However, long-standing experimental assays (4) and recent molecular studies (8,11) have found that changes in multiplicity of infection drastically change the initial decision switch in λ-phage. The experimental evidence indicates that two or more coinfecting λ-phages will lead to lysogeny, whereas a single infecting λ-phage leads to cell lysis (4,8,11). This qualitative change in outcome based on small differences in levels of coinfection may seem counterintuitive, and thus far, lacks a coherent theoretical description. Here we show that when multiple viruses infect the same host cell, nonlinearities in gene regulatory dynamics can lead to qualitative changes in steady-state gene expression, and ultimately to a deterministic outcome, i.e., lysis or lysogeny. This finding suggests that features of viral collective decision switches are inheritable, mutable, and evolvable. The evolvable quantities in this process include the critical multiplicity of infection at which the switch occurs and the ratio of steady-state gene expression for the two different decision states. These features are determined, in part, by kinetic parameters of binding which are easily affected by mutation.

Regulatory model of viral decision processes

Consider a mixture of temperate bacterial viruses and bacterial hosts in which cells are coinfected by $\mathcal{M}$ viruses of an identical strain. A simple model of this situation and a possible mechanism for a viral decision process within a bacterial cell is depicted in Fig. 1. Two genes in this network, x and y, share a common promoter region. When X-dimers are bound to the promoter, they halt transcription of gene y and enhance that of x. When Y-dimers are bound to the promoter, they halt transcription of both genes x and y. Hence, the viral regulatory network includes both a positive and a negative feedback loop (see Table 1 for more details).

Unlike other models in which the copy number remains fixed, here we set the copy number of viral genes equal to the number of coinfecting viruses, $\mathcal{M}$. Following standard

Submitted March 17, 2008, and accepted for publication May 16, 2008.

Address reprint requests to Joshua S. Weitz, Tel.: 404-385-6169; E-mail: jsweitz@gatech.edu.

Editor: Herbert Levine.

0006-3495/08/09/2673/08 $2.00

doi: 10.1529/biophysj.108.133694

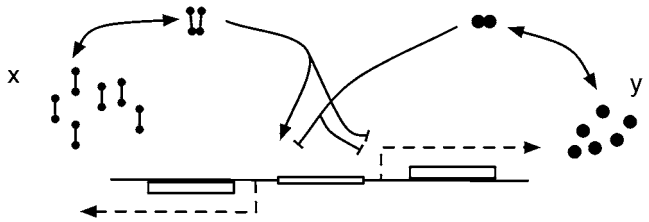

FIGURE 1 Schematic of a bistable switch in which dimers of an excitatory loop (*two circles* with *line*) and an inhibitory loop (*circles*) compete for the same promoter. Solid lines denote protein interactions and dashed lines denote transcriptional events (translation not depicted).

methods (10,17–19), we consider a mass-action model of the dynamics of promoters, mRNA, and proteins. The network is comprised of an excitatory and an inhibitory loop. When promoters are unoccupied, mRNA is transcribed at a rate α_x and α_y for the excitatory and inhibitory loops, respectively. These monomers can dimerize and then bind to the promoter site. When X-dimers are bound, they inhibit transcription of gene y and enhance transcription of gene x at a rate β_x. When Y-dimers are bound, they inhibit transcription of both genes x and y. Following standard methods in the field (10), we track the density of monomers x_1 and y_1, dimers x_2 and y_2, mRNA transcripts m_x and m_y, and promoter occupancies d_0, d_x, and d_y, such that the dynamics are

$$\dot{x}_1 = 2\kappa_- x_2 - 2\kappa_+ x_1^2 + \sigma m_x - \gamma_p x_1, \quad (1)$$

$$\dot{x}_2 = -\kappa_- x_2 + \kappa_+ x_1^2 + k_- d_x - k_+ d_0 x_2, \quad (2)$$

$$\dot{y}_1 = 2\kappa_- y_2 - 2\kappa_+ y_1^2 + \sigma m_y - \gamma_p y_1, \quad (3)$$

$$\dot{y}_2 = -\kappa_- y_2 + \kappa_+ y_1^2 + k_- d_y - k_+ d_0 y_2, \quad (4)$$

$$\dot{d}_0 = k_- d_x + k_- d_y - k_+ d_0 x_2 - k_+ d_0 y_2, \quad (5)$$

$$\dot{d}_x = k_+ d_0 x_2 - k_- d_x, \quad (6)$$

$$\dot{d}_y = k_+ d_0 y_2 - k_- d_y, \quad (7)$$

$$\dot{m}_x = \alpha_x d_0 + \beta_x d_x - \gamma_m m_x, \quad (8)$$

$$\dot{m}_y = \alpha_y d_0 - \gamma_m m_y. \quad (9)$$

In this model, κ_- and κ_+ are the rates of unbinding and dimerization of monomers, k_- and k_+ are the rates of detachment and attachment of dimers to promoter sites, σ is the translational rate, $\alpha_{x,y}$ and β_x are transcriptional rates, γ_m is the degradation rate of transcripts, and γ_p is the degradation rate of proteins. Note that the total concentration of promoter sites remains unchanged, and denote that as $d = \mathcal{M}C$, where $\mathcal{M}$ is the cellular multiplicity of infection and C is a conversion factor corresponding to the molar concentration of a single molecule in a volume equivalent to a bacterial cell, then $d = d_0 + d_x + d_y$ is a constant throughout the dynamics.

TABLE 1 Transcription rates of mRNAs given promoter sites that are unoccupied or occupied by either X- or Y-dimers

Occupancy	x Transcription	y Transcription
None	α_x	α_y
X dimer	β_x	0
Y dimer	0	0

The dimer Y is strictly inhibitory whereas X both represses y and activates itself. When $\alpha_y > \alpha_x$ the inhibitory loop is favored at low $\mathcal{M}$.

In this complete form, mathematical analysis is impractical. Hence, we apply a nonrestrictive quasi-steady-state approximation (QSSA) to the full model (see Appendix 1 for a detailed treatment of this derivation). In the QSSA, we take advantage of the disparity in rates between fast and slow processes in the gene regulatory network and assume that other variables are determined by the slowly varying monomer concentrations. We are able to derive expressions for the rate of change of the rescaled concentrations of X and Y free monomers, denoted here as u and v, respectively,

$$\dot{u} = \mathcal{M}\frac{\alpha_u + \beta_u u^2}{1 + u^2 + v^2} - \gamma_p u, \quad (10)$$

$$\dot{v} = \mathcal{M}\frac{\alpha_v}{1 + u^2 + v^2} - \gamma_p v. \quad (11)$$

The parameters α_u, α_v, and β_u are rescaled rates combining the effects of binding, transcription, translation, and degradation where γ_p is the protein degradation rate (see Appendix 1 for definitions). Importantly, the reformulation of the model shows that changes in the cellular multiplicity of infection, $\mathcal{M}$, directly affect the rates of transcription (in the full model of Eqs. 1–9) and translation (in the protein-only model of Eqs. 10 and 11). Thus, changes in the number of viruses within a cell affect the values of key parameters in a nonlinear dynamic model of regulatory control. Further, predictions of steady-state expression are equivalent whether we are considering the full dynamics of promoters, mRNA, and proteins, or the dynamics of proteins in Eqs. 10 and 11.

The steady-state monomer concentrations in this model, $(\bar{u}, \bar{v})$, can be solved implicitly. After some analysis (see Appendix 1), we find exact expressions for $\mathcal{M}(\bar{u})$ and $\bar{v}(\bar{u})$,

$$\mathcal{M} = \gamma_p \bar{u}\left(\frac{1 + \bar{u}^2}{\alpha_u + \beta_u \bar{u}^2} + \frac{\alpha_v^2 \bar{u}^2}{(\alpha_u + \beta_u \bar{u}^2)^3}\right), \quad (12)$$

$$\bar{v} = \frac{\alpha_v \bar{u}}{\alpha_u + \beta_u \bar{u}^2}. \quad (13)$$

The ratio, $\bar{v}/\bar{u}$, shows the disparity in steady-state expressions and is equivalent to the ratio of the actual concentrations. For low values of $\bar{u}$, $\bar{v}/\bar{u}$ is on the order of α_v/α_u, whereas for large values of $\bar{u}$, $\bar{v}/\bar{u}$ is on the order of $\alpha_v/(\beta_u \bar{u}^2)$. When baseline production of the inhibitory protein exceeds that of the excitatory protein ($\alpha_v > \alpha_u$), the ratio of steady-state expression switches from high to low as $\bar{u}$ increases. This is the key to the origin of collective decision-making in viruses. When $\mathcal{M}$ is low, total expression is kept at low levels and the decision switch favors the inhibitory loop. When $\mathcal{M}$ is large, total expression increases and the decision switch favors the excitatory loop for which the nonlinear positive feedback dominates.

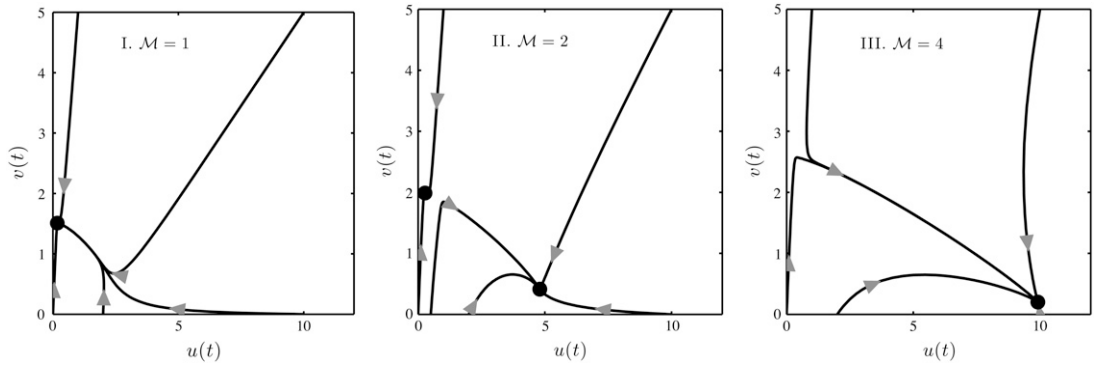

FIGURE 2 Phase plane dynamics of $v(t)$ versus $u(t)$ in the protein-only model of Eqs. 10 and 11 given $\alpha_u = 0.5$, $\alpha_v = 5$, $\beta_u = 2.5$, $\gamma_p = 1$, and $\mathcal{M} = 1$, 2, and 4 respectively. Arrows denote direction of trajectories and solid circles are stable equilibria. From left to right, figures depict the three regimes of the model where dynamics are dominated by the inhibitory pathway (v), contains alternative steady states, and are dominated by the excitatory pathway (u), respectively.

There can be at most three outcomes for this model: 1), an inhibition-dominated regime; 2), a bistable regime; and 3), an excitation-dominated regime (see Fig. 2). These regimes occur for $\mathcal{M} < \mathcal{M}_1$, $\mathcal{M}_1 < \mathcal{M} < \mathcal{M}_2$, and $\mathcal{M} > \mathcal{M}_2$, respectively (see Fig. 3). The critical values, $\mathcal{M}_1$ and $\mathcal{M}_2$, indicate the cellular multiplicity of infection when a change in behavior is expected. We cannot find explicit solutions for $\mathcal{M}_{1,2}$ as a function of the parameters. However, implicit solutions are possible since these critical points satisfy the condition $\partial\mathcal{M}(\bar{u})/\partial\bar{u} = 0$ in Eq. 12. Analysis demonstrates that when $\beta_u \gg \alpha_u$, there must be two critical points where saddle node bifurcations occur (Y. Mileyko, R. I. Joh, and J. S. Weitz, unpublished). First, when $\mathcal{M} = \mathcal{M}_1$, an unstable and stable state emerge. Next, when $\mathcal{M} = \mathcal{M}_2$, the unstable equilibrium collides with the other stable branch. When $\alpha_v > \alpha_u$, there is only one possible steady state for low cellular multiplicity of infection ($\mathcal{M} < \mathcal{M}_1$), where $\bar{v} \gg \bar{u}$. Likewise, there is only one possible steady state for high cellular multiplicity of infection ($\mathcal{M} > \mathcal{M}_2$), where $\bar{u} \gg \bar{v}$. Thus, a cell's fate can be deterministically tuned by, in some cases, the addition or subtraction of a few infecting viruses. In the intermediate regime, $\mathcal{M}_1 < \mathcal{M} < \mathcal{M}_2$, the outcome depends strongly on stochastic effects which may drive the system to one stable expression state or the other. Alternatively, if we had tracked the total concentration of proteins, equal to the sum of monomers, dimers, and bound dimers, we would find the same critical values of $\mathcal{M}$ for bifurcations.

The central elements of this model are the transcriptional feedback and protein dimerization, as has been pointed out in other contexts (18). Without feedback, increases in copy number would not qualitatively change the ratio of gene expression. Without dimerization, the ratio of gene expression would change with varying $\mathcal{M}$, but the change would not be as drastic and there would no longer be a sequence of bifurcations. Given feedback and dimerization, the finding of a sequence of copy-number driven bifurcations are robust to changes in the kinetic parameters. Changes in kinetic parameters will alter features of the copy-number controlled bifurcation, including the critical values of $\mathcal{M}$ where the bifurcations occur and the relative change in expression before and after the bistable regime.

Mechanistic model of the λ-phage initial decision switch

The generic mechanism presented for a deterministically controlled decision switch also applies in more complex scenarios. A simplified version of the lysis-lysogeny switch in λ-phage involving genes *cI*, *cro*, and *cII* is presented in Fig. 4. It is now widely believed that the ultimate fate of the decision process in λ-phage is controlled by CII. High levels

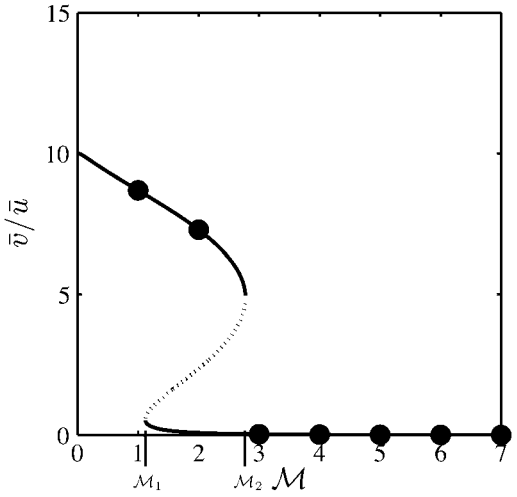

FIGURE 3 Ratio of steady-state protein concentrations for varying cellular multiplicity of infection ($\mathcal{M}$) in the protein-only model of Eqs. 10 and 11 given $\alpha_u = 0.5$, $\alpha_v = 5$, $\beta_u = 2.5$, and $\gamma_p = 1$. Solid lines denote stable branches, dotted line denotes unstable branch, and circles are results of numerical simulations given the initial conditions ($u = 0$, $v = 0$). There are three regimes in this model $\mathcal{M} < \mathcal{M}_1$, $\mathcal{M}_1 < \mathcal{M} < \mathcal{M}_2$, and $\mathcal{M} > \mathcal{M}_2$, where the model is dominated by the inhibitory pathway (v), contains alternative steady states, and is dominated by the excitatory pathway (u), respectively. The critical points $\mathcal{M}_1$ and $\mathcal{M}_2$ correspond to saddle-node bifurcations of the model.

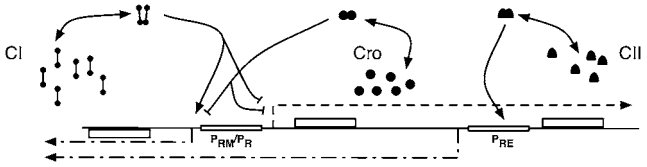

FIGURE 4 Simplified version of the λ-phage switch in which CII acts as a gate protein between the *cI* and the *cro* pathways (3,11). In the schematic, solid lines denote protein interactions, the dashed line denotes transcription events that require no activation, and dashed-solid lines denote transcription events that require activation. More details can be found in Appendix 2.

of CII facilitate production of CI (and the lysogenic pathway) whereas low levels of CII favor production of Cro (and the lytic pathway) (3,8,11,12). The molecular mechanism proposed is that the amount of CII proteins may indirectly measure the number of infecting viruses (8). Despite extensive experimental evidence that increases in coinfection systematically switches a cell's fate from lysis to lysogeny, as yet there is no general theory that explains this process. In particular, why do increases in the copy numbers of viral genes not lead to a proportional increase in the concentration of all components of the regulatory system in a way that their ratios (and hence decisions) are left unchanged?

In the model proposed here, we do not consider the entire λ-phage decision circuit. Rather, we propose a simplified model that captures critical features of the decision switch controlled at multiple promoter sites (3). The two promoter sites considered here are denoted as 1), P_{RM}/P_R and 2), P_{RE} (see Fig. 4 for more details). In addition, CI, Cro, and CII all dimerize before binding. The rules of transcription are as follows: 1), baseline transcription initiates at P_{RM}/P_R to make *cro* and *cII* transcripts; 2), binding of CII at P_{RE} leads to transcription of *cI*; 3), binding of CI at P_{RM}/P_R catalyzes transcription of *cI* and inhibits transcription of *cro* and *cII*; and 4), binding of Cro at P_{RM}/P_R inhibits transcription of all genes. In reality, the P_{RM} and P_R promoters are distinct and comprised of an overlapping set of three operator regions, which we ignore in the interest of analytic tractability (3,20, 21).

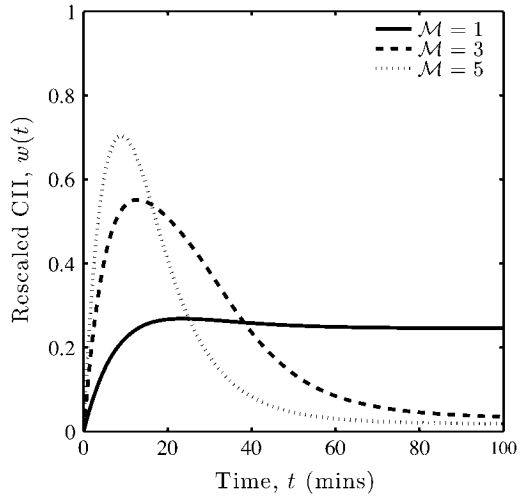

FIGURE 5 Simulated dynamics of the decision switch as a function of multiplicity of infection, where $\mathcal{M} = 1$, 3, and 5. Notice that CII functions as a gating protein. Increases in $\mathcal{M}$ shift CII above a critical threshold enabling transcription of *cI* and coupling to the nonlinear positive feedback loop. Values of rescaled parameters used in the numerical simulations are $\beta_u = 0.08$, $\delta_u = 0.06$, $\alpha_v = 0.04$, $\alpha_w = 0.04$, $\gamma_u = 0.04$, $\gamma_v = 0.05$, and $\gamma_w = 0.12$ all in units of min^{-1}. More details can be found in Appendix 2.

We model this system, as before, by tracking the dynamics of promoter, mRNA and protein concentrations. A full list of dynamical expressions and parameter values can be found in Appendix 2. As in the generic model, we derive equations approximating the dynamics of protein concentration. Denoting u, v, and w as the rescaled concentrations of CI, Cro, and CII monomers, we find the rates of change to be

$$\dot{u} = \mathcal{M}\frac{\beta_u u^2}{1+u^2+v^2} + \mathcal{M}\frac{\delta_u w^2}{1+w^2} - \gamma_u u, \tag{14}$$

$$\dot{v} = \mathcal{M}\frac{\alpha_v}{1+u^2+v^2} - \gamma_v v, \tag{15}$$

$$\dot{w} = \mathcal{M}\frac{\alpha_w}{1+u^2+v^2} - \gamma_w w, \tag{16}$$

where $\mathcal{M}$ is, as before, the cellular multiplicity of infection and the rescaled variables are defined in Appendix 2.

The values of these rescaled parameters depend on kinetic rates, some of which have been studied in the literature while others have not. Generically, the CI-CII-Cro model undergoes a series of saddle-node bifurcations that go from a stable regime where Cro dominates ($\bar{v} > \bar{u}$) to a bistable regime and back to a stable regime where CI dominates ($\bar{u} > \bar{v}$). CII acts as a gate protein in this system. Increasing $\mathcal{M}$ drives the dynamic level of w past a critical point where the nonlinearity of the positive feedback in CI production leads to a switch in behavior (see Figs. 5 and 6). These results are robust to small changes in the values of parameters, and so many of the values in the regulatory network could be changed and the switch would still function. As in the previous case, the system possesses only one steady state given suitably low or high levels of coinfection. Hence, the switch is dominated by deterministic behavior in contrast to suggestions that decision outcomes must have stochastic origins or be driven by changes in environmental conditions (6).

Parameters are chosen (see Appendix 2) such that maximal transcriptional rates are on the order of a few transcripts per minute per gene, maximal translation rates are on the order of one protein for every few minutes per transcript, dissociation constants are on the order of 10^7 M^{-1}, and mRNA and protein degradation rates are on the order of 0.1 per min (6,7,16,20). Figs. 5 and 6 demonstrate that these parameter values can lead to a CDM-driven switch where lysis is favored at $\mathcal{M} = 1$ and lysogeny is favored at $\mathcal{M} \geq 2$ in agreement with observations (3,4,8). Peak concentrations of CI and Cro are of the same magnitude as experimental observations (in the hundreds of molecules) (3). Quantitative deviations are unsurprising, given the uncertainty in param-

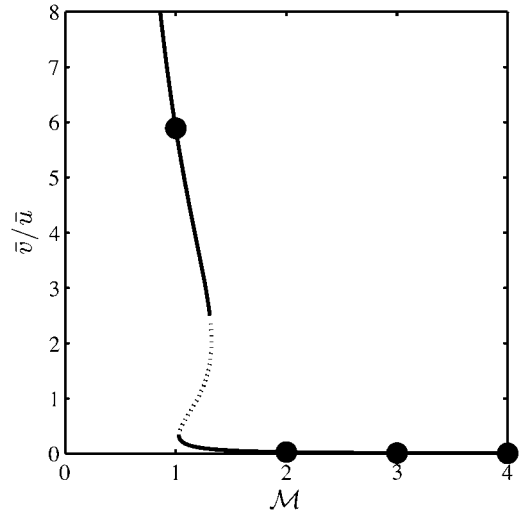

FIGURE 6 Bifurcation diagram for $\bar{v}/\bar{u}$ as a function of $\mathcal{M}$ where solid line is analytical curve and circles are from numerical simulations of Eqs. 14–16 given the initial conditions ($u = 0$, $v = 0$, $w = 0$). Values of rescaled parameters are the same as those used in Fig. 5.

eters and the reduction of network complexity as compared to the hypothesized λ-phage switch. The relationship between kinetic parameters and features of a genetic switch controlled by copy number, including the width of the bistable regime and the difference in the steady-state expression of the two bistable states, are explored in a separate work (Y. Mileyko, R. I. Joh, and J. S. Weitz, unpublished). Note also in this model, if the degradation rate of CI is increased suddenly, as occurs after a cell experiences DNA damage, then the lysogenic state becomes unstable in agreement with experiments (3) and other numerical studies (7,10,16,22).

DISCUSSION

Living organisms exhibit a remarkable range of complex group behaviors (23–25). Often, the number of individuals is a key factor in determining when and if the group exhibits functions and/or behaviors distinct from those of individuals (24–27). Although viruses are one of the few types of organisms for which collective decision making has not yet been proved, we have demonstrated a mechanism by which they may do so. The finding that multiple infections can change behavior within a cell indicates that viral infections are not static, but rather may react to their own dynamics. This response is, in principle, an evolvable life history trait of bacterial viruses conferring some selective benefit to strains which adopt this strategy. The ecological circumstances favoring lysogeny have been addressed previously, though the issue is far from settled (28). Although λ-phage often constitutes the dogma for how a temperate phage behaves, mutations that lead to changes in network structure, degree of cooperativity, and kinetic rates could lead to qualitative shifts in the exploitation strategy of a host (8). Viruses could kill at low $\mathcal{M}$ and go latent at high $\mathcal{M}$, or vice versa, depending on binding parameters in the regulatory feedback loops controlling a cell's fate. Virulent bacteriophages differ in their life history traits (such as burst size or virion decay rate) by multiple orders of magnitude (29), which suggests that diverse life history strategies may be found in temperate bacteriophages as well. Indeed, observations of λ-phage mutants have already shown that decision variants may in fact be engineered (30,31).

There are many challenges remaining in the study of CDM in bacterial viruses. First, the dynamics of intracellular mRNAs and proteins are stochastic, and we are in the process of evaluating stochastic versions of the current models to evaluate the likelihood of chance outcomes in a deterministically driven decision system. Next, the infection of a host cell is rarely simultaneous. Therefore, the subsequent infection by viruses leads to discrete shifts in dynamics and in the parameters controlling the unfolding of exploitation. In that sense, the ecological dynamics of infection and the intracellular dynamics of decision making are necessarily coupled. To what extent subsequent viruses can change the outcome of a previously infected, but not yet committed, virus remains an open question. Finally, the decision-switch we presented is a simplification of many complex intracellular processes. Analyses of the decision switch that incorporate additional biological realism should retain the feature of sensitivity to $\mathcal{M}$. We expect that our finding of nonlinear copy number effects will remain a necessary part of subsequent models.

Experimental tests of the effect of multiplicity of infection on the lysis-lysogeny switch have been conducted using plate-based assays at the population level (4) and using expression fluorescence assays of synchronously infected cell ensembles (8). We believe that single-cell experiments are necessary to test the nonlinear effect of copy number on decision outcome (32,33). Simultaneous measurements of viral coinfection level and expression dynamics will facilitate unambiguous determination of the link between $\mathcal{M}$ and the genetic cascade leading to lysis or lysogeny. Already, experimental monitoring of single-cell expression dynamics has provided insight into the sequence of events that allow the λ-prophage to induce upon UV irradiation (32). Copy number variation may affect the initial decision switch as well as prophage induction. For example, variation in physiological state will lead to dynamic changes in the number of chromosomes within a lysogen. Such dynamic changes could modify rates of viral gene expression affecting prophage function in the presence and absence of cell stress (15).

The choice of whether to burst from a cell or to remain/enter a latent state is a key feature of viruses from phages to human pathogens. The cellular multiplicity of infection may well play a role in shaping other viral decision processes, even if the genetic details are different. At the very least, we have shown here that small changes in coinfection are a sufficient determinant of the initial lysis versus lysogeny

switch upon infection. More generally, our findings suggest that other gene regulatory modules may depend sensitively on copy number, by modifying kinetic rates of transcription within a nonlinear dynamical system.

APPENDIX 1: BISTABLE SWITCH DYNAMICS USING A QUASI-STEADY-STATE APPROXIMATION

Consider a model of viral exploitation in which two competing regulatory pathways share a common promoter. The network is comprised of an excitatory and an inhibitory loop as described in the main text. We assume that translation and transcription are the slow processes in the model and binding and dimerization are fast. Hence, variables x_2, y_2, d_x, d_y, and d_0 are changing much faster than the rest. Therefore, we obtain a quasi-steady-state approximation (QSSA) of the full system by setting the corresponding derivatives to zero:

$$0 = -\kappa_- x_2 + \kappa_+ x_1^2 + k_- d_x - k_+ d_0 x_2, \tag{17}$$

$$0 = -\kappa_- y_2 + \kappa_+ y_1^2 + k_- d_y - k_+ d_0 y_2, \tag{18}$$

$$0 = k_+ d_0 x_2 - k_- d_x, \tag{19}$$

$$0 = k_+ d_0 y_2 - k_- d_y. \tag{20}$$

Since we are interested in steady states in this model we omit a more careful treatment of prefactors involved with this QSSA as presented elsewhere (10). Adding Eqs. 17 and 19, 18 and 20 we obtain

$$0 = -\kappa_- x_2 + \kappa_+ x_1^2, \tag{21}$$

$$0 = -\kappa_- y_2 + \kappa_+ y_1^2, \tag{22}$$

which implies that

$$x_2 = c_p x_1^2, \tag{23}$$

$$y_2 = c_p y_1^2, \tag{24}$$

where $c_p = \kappa_+/\kappa_-$.

Recall that the total concentration of promoter sites remains unchanged, hence $d = d_0 + d_x + d_y$ is a constant throughout the dynamics. After some algebra we find that

$$d_x = d\frac{c_p c_d x_1^2}{1 + c_p c_d(x_1^2 + y_1^2)}, \tag{25}$$

$$d_y = d\frac{c_p c_d y_1^2}{1 + c_p c_d(x_1^2 + y_1^2)}, \tag{26}$$

$$d_0 = \frac{d}{1 + c_p c_d(x_1^2 + y_1^2)}, \tag{27}$$

where $c_d = k_+/k_-$.

Thus, the quasi-steady-state approximation for the system has the following form:

$$\dot{x}_1 = \sigma m_x - \gamma_p x_1, \tag{28}$$

$$\dot{y}_1 = \sigma m_y - \gamma_p y_1, \tag{29}$$

$$\dot{m}_x = d\frac{\alpha_x + \beta_x c_p c_d x_1^2}{1 + c_p c_d(x_1^2 + y_1^2)} - \gamma_m m_x, \tag{30}$$

$$\dot{m}_y = d\frac{\alpha_y}{1 + c_p c_d(x_1^2 + y_1^2)} - \gamma_m m_y. \tag{31}$$

We simplify the system further by assuming transcription is faster than translation. Setting the derivatives of m_x and m_y to zero yields

$$m_x = \frac{d}{\gamma_m}\frac{\alpha_x + \beta_x c_p c_d x_1^2}{1 + c_p c_d(x_1^2 + y_1^2)} \tag{32}$$

$$m_y = \frac{d}{\gamma_m}\frac{\alpha_y}{1 + c_p c_d(x_1^2 + y_1^2)}. \tag{33}$$

Substituting these expressions into the equations for x_1 and y_1 we get the following system:

$$\dot{x}_1 = \frac{d\sigma}{\gamma_m}\frac{\alpha_x + \beta_x c_p c_d x_1^2}{1 + c_p c_d(x_1^2 + y_1^2)} - \gamma_p x_1, \tag{34}$$

$$\dot{y}_1 = \frac{d\sigma}{\gamma_m}\frac{\alpha_y}{1 + c_p c_d(x_1^2 + y_1^2)} - \gamma_p y_1. \tag{35}$$

We then rescale the variables: $u = \sqrt{c_p c_d}x_1$, $v = \sqrt{c_p c_d}y_1$, and set $\beta_u = C\beta_x\sigma\sqrt{c_p c_d}/\gamma_m$, $\alpha_u = C\alpha_x\sigma\sqrt{c_p c_d}/\gamma_m$, and $\alpha_v = C\alpha_y\sigma\sqrt{c_p c_d}/\gamma_m$. The dynamics of the rescaled expression are

$$\dot{u} = \mathcal{M}\frac{\alpha_u + \beta_u u^2}{1 + u^2 + v^2} - \gamma_p u, \tag{36}$$

$$\dot{v} = \mathcal{M}\frac{\alpha_v}{1 + u^2 + v^2} - \gamma_p v. \tag{37}$$

where, as noted before, $\mathcal{M} = d/C$ is the copy number of viral genes. This system can be thought of as a protein-only model of the switch.

Continuing our derivation of steady states, we set the above derivatives to zero:

$$0 = \mathcal{M}\frac{\alpha_u + \beta_u u^2}{1 + u^2 + v^2} - \gamma_p u, \tag{38}$$

$$0 = \mathcal{M}\frac{\alpha_v}{1 + u^2 + v^2} - \gamma_p v. \tag{39}$$

The second equation implies that

$$\frac{\mathcal{M}}{1 + u^2 + v^2} = \frac{\gamma_p}{\alpha_v}v. \tag{40}$$

Substituting this expression into the first equation, we get

$$\frac{\gamma_p}{\alpha_v}v(\alpha_u + \beta_u u^2) = \gamma_p u \Rightarrow \bar{v} = \frac{\alpha_v \bar{u}}{\alpha_u + \beta_u \bar{u}^2}. \tag{41}$$

From this, we can now find the expression for $\mathcal{M}$ as a function of $\bar{u}$:

$$\mathcal{M} = \gamma_p \bar{u}\left(\frac{1 + \bar{u}^2}{\alpha_u + \beta_u \bar{u}^2} + \frac{\alpha_v^2 \bar{u}^2}{(\alpha_u + \beta_u \bar{u}^2)^3}\right). \tag{42}$$

This function defines implicit dependence of $\bar{u}$ on $\mathcal{M}$. We can find values of $\mathcal{M}$ at which $\partial\mathcal{M}(\bar{u})/\partial\bar{u} = 0$, which correspond to critical values where qualitative changes in steady-state expression are expected. We only consider monomer degradation in this and the subsequent model in Appendix 2. Assuming only monomers degrade, only dimers degrade, or some combination of those scenarios does not change any of the qualitative features of our results.

APPENDIX 2: DYNAMICS OF CI-CII-CRO

The dynamics of the CI-CII-Cro system as depicted in Fig. 4 of the main text are:

$$\dot{x}_1 = 2\kappa_-^{(x)} x_2 - 2\kappa_+^{(x)} x_1^2 + \sigma m_x - \gamma_x x_1, \tag{43}$$

$$\dot{x}_2 = -\kappa_-^{(x)} x_2 + \kappa_+^{(x)} x_1^2 + k_-^{(x)} d_x - k_+^{(x)} d_0 x_2, \tag{44}$$

$$\dot{y}_1 = 2\kappa_-^{(y)} y_2 - 2\kappa_+^{(y)} y_1^2 + \sigma m_y - \gamma_y y_1, \tag{45}$$

$$\dot{y}_2 = -\kappa_-^{(y)} y_2 + \kappa_+^{(y)} y_1^2 + k_-^{(y)} d_y - k_+^{(y)} d_0 y_2, \tag{46}$$

$$\dot{z}_1 = 2\kappa_-^{(z)} z_2 - 2\kappa_+^{(z)} z_1^2 + \sigma m_z - \gamma_z z_1, \tag{47}$$

$$\dot{z}_2 = -\kappa_-^{(z)} z_2 + \kappa_+^{(z)} z_1^2 + k_-^{(z)} e_z - k_+^{(z)} e_0 z_2, \tag{48}$$

$$\dot{d}_0 = k_-^{(x)} d_x + k_-^{(y)} d_y - k_+^{(x)} d_0 x_2 - k_+^{(y)} d_0 y_2, \tag{49}$$

$$\dot{d}_x = k_+^{(x)} d_0 x_2 - k_-^{(x)} d_x, \tag{50}$$

$$\dot{d}_y = k_+^{(y)} d_0 y_2 - k_-^{(y)} d_y, \tag{51}$$

$$\dot{e}_0 = -k_+^{(z)} e_0 z_2 + k_-^{(z)} e_z, \tag{52}$$

$$\dot{e}_z = k_+^{(z)} e_0 z_2 - k_-^{(z)} e_z, \tag{53}$$

$$\dot{m}_x = \beta_x d_x + \delta_x e_z - \gamma_m m_x, \tag{54}$$

$$\dot{m}_y = \alpha_y d_0 - \gamma_m m_y, \tag{55}$$

$$\dot{m}_z = \alpha_z d_0 - \gamma_m m_z. \tag{56}$$

Using a sequence of quasi-steady-state approximations in which we integrate over processes of dimerization, binding, and mRNA production, the model can be reduced to a protein-only dynamic model of x, y, and z monomer concentration. Here we relax the assumption that dimerization and binding constants are identical for each protein. In analogy to the two-protein system derived in the main text, the model equations are

$$\dot{x} = \frac{\mathcal{M}C\beta_x\sigma/\gamma_m (c_p^{(x)} c_d^{(x)} x^2)}{1 + c_p^{(x)} c_d^{(x)} x^2 + c_p^{(y)} c_d^{(y)} y^2} + \frac{\mathcal{M}C\delta_x\sigma/\gamma_m (c_p^{(z)} c_d^{(z)} z^2)}{1 + c_p^{(z)} c_d^{(z)} z^2} - \gamma_x x, \tag{57}$$

$$\dot{y} = \frac{\mathcal{M}C\alpha_y\sigma/\gamma_m}{1 + c_p^{(x)} c_d^{(x)} x^2 + c_p^{(y)} c_d^{(y)} y^2} - \gamma_y y, \tag{58}$$

$$\dot{z} = \frac{\mathcal{M}C\alpha_z\sigma/\gamma_m}{1 + c_p^{(x)} c_d^{(x)} x^2 + c_p^{(y)} c_d^{(y)} y^2} - \gamma_z z, \tag{59}$$

where $c_p^{(x)} = \kappa_+^{(x)}/\kappa_-^{(x)}$, $c_d^{(x)} = k_+^{(x)}/k_-^{(x)}$, and likewise for y and z. In addition, here $\mathcal{M}$ denotes the integer multiplicity of infection and C is the conversion factor for representing operator concentrations in molar units. As before, the number of promoter sites are given as

$$d_0 + d_x + d_y = e_0 + e_z = \mathcal{M}C. \tag{60}$$

Note that converting from concentrations to estimates of molecules per cell has been calibrated based on an assumption of cell volumes on the order of $1-2\times10^{-15}$ L. Hence, the number of molecules in a bacterial cell is equal to the molar concentration divided by C. The dynamic factors involved in tracking the total protein concentration have been studied for the quasi-steady-state approximation in other contexts (10). Importantly, they do not alter the predictions regarding steady-state behavior.

We propose the following rescaling of this model: $u = \sqrt{c_p^{(x)} c_d^{(x)}}\, x_1$, $v = \sqrt{c_p^{(y)} c_d^{(y)}}\, y_1$, $w = \sqrt{c_p^{(z)} c_d^{(z)}}\, z_1$, $\beta_u = C\beta_x\sigma\sqrt{c_p^{(x)} c_d^{(x)}}/\gamma_m$, $\delta_u = C\delta_x\sigma\sqrt{c_p^{(x)} c_d^{(x)}}/\gamma_m$, $\alpha_v = C\alpha_y\sigma\sqrt{c_p^{(y)} c_d^{(y)}}/\gamma_m$, $\alpha_w = C\alpha_z\sigma\sqrt{c_p^{(z)} c_d^{(z)}}/\gamma_m$, $\gamma_u = \gamma_x$, $\gamma_v = \gamma_y$, and $\gamma_w = \gamma_z$. Using this rescaling we recover the model in Eqs. 14–16 in the main text. Parameter estimates are approximate. They are in range with experimental measurements and typical values for dimerization, binding, transcription, translation and degradation in bacteria and viruses. The approximate kinetic values are as follows (7,16,20): $c_p^{(x)} \approx 10^7$ M^{-1}, $c_p^{(y)} \approx 10^7$ M^{-1}, $c_p^{(z)} \approx 10^7$ M^{-1}, $c_d^{(x)} \approx 10^7$ M^{-1}, $c_d^{(y)} \approx 10^7$ M^{-1}, $c_d^{(z)} \approx 10^7$ M^{-1}, $\beta_x \approx 1.6$ min^{-1}, $\delta_x \approx 1.2$ min^{-1}, $\alpha_y \approx 0.8$ min^{-1}, $\alpha_z \approx 0.8$ min^{-1}, $\sigma \approx 0.5$ min^{-1}, $\gamma_m \approx 0.1$ min^{-1}, $\gamma_x \approx 0.04$ min^{-1}, $\gamma_y \approx 0.05$ min^{-1}, $\gamma_z \approx 0.12$ min^{-1}, and $C \approx 10^{-9}$ M. Here the degradation of CII is higher than either CI or Cro, in part due to the instability of the protein and the need for other components such as CIII that prevent its degradation by bacterial proteases (3). Importantly, model behaviors are robust to small changes in these parameters, and, in particular, to changes in the rescaled values of β_u, δ_u, α_v, α_w, and the degradation rates $\gamma_{u,v,w}$.

The authors thank J. Dushoff for many helpful conversations and S. Spiro, M. Goodisman, and I. Golding for their comments on the manuscript.

J.S.W. is pleased to acknowledge the support of the Defense Advanced Research Projects Agency under grant No. HR0011-05-1-0057 to Princeton University. This work was supported in part by a Molecular and Cellular Biosciences grant from National Science Foundation (E.O.V., Principal Investigator). Joshua S. Weitz, PhD, holds a Career Award at the Scientific Interface from the Burroughs Wellcome Fund.

Any opinions, findings, and conclusions or recommendations expressed in this material are those of the authors and do not necessarily reflect the views of the sponsoring institutions.

REFERENCES

1. Dimmock, N. J., A. J. Easton, and K. N. Leppard. 2007. Introduction to Modern Virology, 5th Ed. Blackwell Publishing, Malden, MA.
2. Calendar, R. Editor. 2005. The Bacteriophages. Oxford University Press, New York.
3. Ptashne, M. 2004. A Genetic Switch: Phage Lambda Revisited, 3rd Ed. Cold Spring Harbor Laboratory Press, Cold Spring Harbor, NY.
4. Kourilsky, P. 1973. Lysogenization by bacteriophage-λ. 1. Multiple infection and lysogenic response. *Mol. Gen. Genet.* 122:183–195.
5. Herskowitz, I., and D. Hagen. 1980. The lysis-lysogeny decision of phage λ: explicit programming and responsiveness. *Annu. Rev. Genet.* 14:399–445.
6. Arkin, A., J. Ross, and H. H. McAdams. 1998. Stochastic kinetic analysis of developmental pathway bifurcation in phage λ-infected *Escherichia coli* cells. *Genetics.* 149:1633–1648.
7. Aurell, E., S. Brown, J. Johanson, and K. Sneppen. 2002. Stability puzzles in phage λ. *Phys. Rev. E Stat. Nonlin. Soft Matter Phys.* 65: 051914.
8. Kobiler, O., A. Rokney, N. Friedman, D. L. Court, J. Stavans, and A. B. Oppenheim. 2005. Quantitative kinetics analysis of the bacteriophage λ genetic network. *Proc. Natl. Acad. Sci. USA.* 102:4470–4475.
9. Oppenheim, A. B., O. Kobiler, J. Stavans, D. Court, and S. Adhya. 2005. Switches in bacteriophage-λ development. *Annu. Rev. Genet.* 39: 409–429.
10. Bennett, M. R., D. Volfson, L. Tsimring, and J. Hasty. 2007. Transient dynamics of genetic regulatory networks. *Biophys. J.* 92: 3501–3512.
11. Court, D. L., A. B. Oppenheim, and S. L. Adhya. 2007. A new look at bacteriophage λ genetic networks. *J. Bacteriol.* 189:298–304.

12. Kobiler, O., A. Rokney, and A. B. Oppenheim. 2007. Phage-λ CIII: a protease inhibitor regulating the lysis-lysogeny decision. *PLoS One*. 2:e363.

13. Murray, N. E., and A. Gann. 2007. What has phage-λ ever done for us? *Curr. Biol.* 17:R305–R312.

14. Dodd, I. B., K. E. Shearwin, and J. B. Egan. 2005. Revisited gene regulation in bacteriophage λ. *Curr. Opin. Genet. Dev.* 15:145–152.

15. Rokney, A., O. Kobiler, A. Amir, D. L. Court, J. Stavans, S. Adhya, and A. B. Oppenheim. 2008. Host responses influence on the induction of λ-prophage. *Mol. Microbiol.* 68:29–36.

16. Santillán, M., and M. C. Mackey. 2004. Why the lysogenic state of phage λ is so stable: a mathematical modeling approach. *Biophys. J.* 86:75–84.

17. McAdams, H. H., and A. Arkin. 1997. Stochastic mechanisms in gene expression. *Proc. Natl. Acad. Sci. USA*. 94:814–819.

18. Cherry, J. L., and F. R. Adler. 2000. How to make a biological switch. *J. Theor. Biol.* 203:117–133.

19. Hasty, J., D. McMillen, F. Isaacs, and J. J. Collins. 2001. Computational studies of gene regulatory networks: *in numero* molecular biology. *Nat. Rev. Genet.* 2:268–279.

20. Ackers, G. K., A. D. Johnson, and M. A. Shea. 1982. Quantitative model for gene regulation by λ phage repressor. *Proc. Natl. Acad. Sci. USA*. 79: 1129–1133.

21. Shea, M. A., and G. K. Ackers. 1985. The OR control system of bacteriophage-λ. A physical chemical model of gene regulation. *J. Mol. Biol.* 181:211–230.

22. Tian, T., and K. Burrage. 2004. Bistability and switching in the lysis/lysogeny genetic regulatory network of bacteriophage-λ. *J. Theor. Biol.* 227:229–237.

23. Camazine, S., J. Sneyd, and T. D. Seeley. 1991. Collective decision-making in honey-bees—how colonies choose among nectar sources. *Behav. Ecol. Sociobiol.* 28:277–290.

24. Miller, M. B., and B. L. Bassler. 2001. Quorum sensing in bacteria. *Annu. Rev. Microbiol.* 55:165–199.

25. West, S. A., A. S. Griffin, A. Gardner, and S. P. Diggle. 2006. Social evolution theory for microorganisms. *Nat. Rev. Microbiol.* 4:597–607.

26. Vicsek, T., A. Czirók, E. Ben-Jacob, I. Cohen, and O. Schochet. 1995. Novel type of phase transition in a system of self-driven particles. *Phys. Rev. Lett.* 75:1226–1229.

27. Couzin, I. D., J. Krause, N. R. Franks, and S. A. Levin. 2005. Effective leadership and decision-making in animal groups on the move. *Nature*. 433:513–516.

28. Stewart, F. M., and B. R. Levin. 1984. The population biology of bacterial viruses: why be temperate. *Theor. Popul. Biol.* 26:93–117.

29. De Paepe, M., and F. Taddei. 2006. Viruses' life history: towards a mechanistic basis of a trade-off between survival and reproduction among phages. *PLoS Biol.* 4:e193.

30. Little, J. W., D. P. Shepley, and D. W. Wert. 1999. Robustness of a gene regulatory circuit. *EMBO J.* 18:4299–4307.

31. Atsumi, S., and J. W. Little. 2006. A synthetic phage λ regulatory circuit. *Proc. Natl. Acad. Sci. USA*. 103:19045–19050.

32. Amir, A., O. Kobiler, A. Rokney, A. B. Oppenheim, and J. Stavans. 2007. Noise in timing and precision of gene activities in a genetic cascade. *Mol. Sys. Biol.* 3:71.

33. Baek, K., S. Svenningsen, H. Eisen, K. Sneppen, and S. Brown. 2003. Single-cell analysis of λ immunity regulation. *J. Mol. Biol.* 334: 363–372.